Nonuniform output characteristics of laser diode with wet-etched spot-size converter

Joong-Seon Choe, Yong-Hwan Kwon, Sung-Bock Kim, and Jung Jin Ju

Electronics and Telecommunications Research Institute, Daejeon 305-700, Korea

jschoe@etri.re.kr

Abstract: We study the output characteristics of spot-size converter (SSC) integrated buried heterostructure (BH) laser diode (LD) by forming SSC with wet etching process. SSC-LD shows large chip-to-chip variation in threshold current(I_{th}) and slope efficiency (η_{slope}) compared to LD without SSC. I_{th} and η_{slope} are closely related with each other so that the front facet η_{slope} increases while the rear facet η_{slope} decreases with I_{th}. Far-field angle is also found to be proportional to the front facet η_{slope}. The trends observed are explained clearly by a unidirectional loss occurring when photons travel from the front to rear facet.

OCIS codes: (250.5960) Semiconductor lasers, (250.5590) Quantum-well, -wire and -dot devices.

References and links

1. Y.-H. Kwon, J.-S. Choe, J. Kim, K. Kim, K.-S. Choi, B.-S. Choi, and H. Yun, "Fabrication of 40 Gb/s front-end optical receivers using spot-size converter integrated waveguide photodiodes," ETRI Journal **27**(5), 484–490 (2005).
2. H. Oohashi, M. Fukuda, Y. Kondo, M. Wada, Y. Tohmori, Y. Sakai, H. Toda, and Y. Itaya, "Reliability of 1300-nm spot-size converter integrated laser diodes for low-cost optical modules in access networks," J. Lightwave Technol. **16**, 1302–1307 (1998).
3. Y. Itaya, Y. Tohmori, and H. Toba, "Spot-size converter integrated laser diodes (SS-LDs)," IEEE J. Select Topics Quantum Electron. **3**(3), 968–974 (1997).
4. H. S. Cho, K. H. Park, J. K. Lee, D. H. Jang, J. S. Kim, K. S. Park, C. S. Park, and K. E. Pyun, "Unbalanced facet output power and large spot size in 1.3 μm tapered active stripe lasers," Electron. Lett. **33**(9), 781–782 (1997).
5. S.-W. Ryu, S.-B. Kim, J.-S. Sim, and J. Kim, "1.55-μm spot-size converter integrated laser diode with conventional buried-heterostructure laser process," IEEE Photon. Technol. Lett. **15**(1), 12–14 (2003).
6. A. Lestra and J.-Y. Emery, "Monolithic integration of spot-size converters with 1.3-μm lasers and 1.55-μm polarization insensitive semiconductor optical amplifiers," IEEE J. Select Topics Quantum Electron. (1997).
7. B. T. Lee, R. A. Logan, R. F. Kalicek, Jr., A. M. Sergent, D. L. Coblentz, K. W. Wecht, and T. Tanbun-Ek, "Fabrication of InGaAsP/InP buried heterostructure laser using reactive ion etching and metalorganic chemical vapor deposition," IEEE Photon. Technol. Lett. **5**(33), 279–281 (1993).
8. W.-C. W. Fang, C. G. Bethea, Y. K. Chen, and S. L. Chuang, "Longitudinal spatial inhomogeneities in high-power semiconductor lasers," IEEE J. Selected Topic. Quantum Electron. **1**(2), 117–127 (1995).
9. G. P. Agrawal and N. K. Dutta, *Semiconductor Lasers*, 2nd ed. (Van Nostrand Reinhold, New York, 1993).

1. Introduction

Laser diodes (LD's) are widely used in many fields as coherent light sources. While application area covers laser display, optical pickup, and biomedical diagnostics, the main usage of LD is still signal source in optical communication[1]. Conventional edge emitting LD has large far-field angle about 30° that causes poor coupling efficiency with a single-mode fiber. In order to reduce the coupling loss, several methods are used such as integration of spot-size converter

(SSC), insertion of microlens between LD and fiber, and using a tapered fiber. Among them, the integration of SSC in LD is the most attractive in that it is cost-effective and efficient in improving mode matching [2].

SSC integrated LD (SSC-LD) is composed of light-generating and mode-converting part. Optical mode generated and amplified in the former gets large in size propagating along the latter for narrower far-field. Mode-converting part has vertical or lateral taper that transfers the mode of active waveguide to passive waveguide [3].

In SSC-LD, the slope efficiency (η_{slope}) of the front facet (η_{front}) is generally larger than that of the rear facet (η_{rear}) [4, 5]. It was shown that the difference in η_{slope} is caused by unidirectional loss that occurs when light propagates along the direction from SSC to the rear facet [6]. According to Ref. [6], η_{slope} would be equal for both the facets if the mode transition occurs adiabatically. Therefore the slope efficiency ratio (SER) $\eta_{\text{front}}/\eta_{\text{rear}}$ can be a figure of merit for evaluating SSC as well as far-field angle.

The taper formation requires patterning and etching of the taper tip. Minute parts like SSC taper are much influenced if a deviation is generated during the process. In SSC-LD, wet process is usually adopted for the active region etching because it produces better etching sidewall adequate for growing current block layers in buried heterostructure (BH) LD [7]. However, wet etching is generally apt to result in inhomogeneous etching depth over the wafer and nonuniform device characteristics. Dry etching is better in uniformity, but not adequate if epitaxial regrowth should follow.

In this study, SSC-LD with lateral wet-etched taper was fabricated. SSC fabrication process produced wide device performance variation, observed in output characteristics. This paper discusses the correlation between the output characteristics of η_{slope}, threshold current (I_{th}), and far-field angle.

2. Experiment

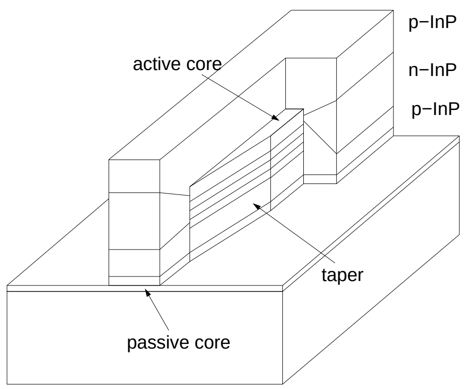

Fig. 1. Schematic structure of 1.3μm SSC-LD. The structure is similar to that of conventional BH LD except for the active region etched to taper shape and passive core beneath the lower cladding layer.

Figure 1 shows the schematic structure diagram of the SSC-LD fabricated. Fabrication process begins by metalorganic chemical vapor depsition growth of epitaxial layers including quantum wells ($\lambda = 1.3\mu$m), passive waveguide, and lower cladding layer. After the first growth, the active region pattern with taper is formed though the conventional photolithography process. The tip width of the taper on the mask image is designed 0.7μm in consideration of the undercut during wet etching.

Active region was etched by $HBr:H_2O_2:H_2O$=16:4:100 solution. HBr solution is widely used in BH LD fabrication process due to its clear etching sidewall and low etching selectivity [7].

After the wafer was etched in the active region including taper, *p*-*n*-*p* current blocking layers, upper cladding, and *p*-contact layer were grown successively. Ridge dry etching, polyimide passivation, *p*-metal evaporation, lapping, *n*-metal evaporation, and cleaving process completed the fabrication. The devices with 600μm length were composed of 300-μm-long non-tapered region, 250-μm-long tapered region, and 50-μm-long passive region.

The characterization of the devices were performed in chip bars. The current-output (I-L) characteristics were measured using integrating sphere in order to rule out coupling loss. Current source operated under pulsed-mode ($t_{\text{on}} = t_{\text{off}} = 50\mu$sec) and the temperature of the device stage was set at 25°C.

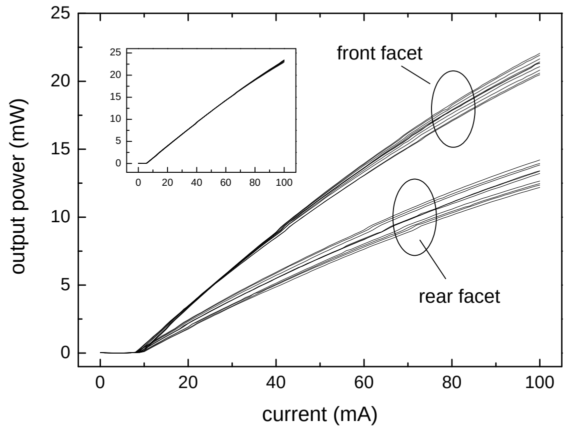

Fig. 2. I-L characteristics of SSC-LD's in a chip bar. As previously reported [4, 5], the slope efficiency from the front facet with SSC is larger than that from the rear facet. Inset is the data for LD's without SSC. Comparing the two data, I-L curves of SSC-LD show larger spread.

3. Result

Figure 2 shows I-L data of SSC-LD's in a chip bar. Although the devices were located close to each other in the wafer, I-L characteristic shows large variation both in η_{slope} and I_{th}. The deviation is so large that the output power from the front facet varies from 20 to 22 mW at 100 mA. Compared with SSC-LD, nearly the same performance was observed from LD's without SSC and the output power deviation is as small as 0.5 mW at 100 mA, as in inset of Fig.2. This shows that material inhomogeneity or etching depth difference for the LD active region does not affect much the LD performance.

SSC-LD has SSC and passive waveguide as well as conventional LD part. Therefore those additive parts of SSC-LD are the origin of the chip-to-chip performance deviation. SSC transfers optical mode from active/passive waveguide to passive/active waveguide with its adiabatically varying effective index. The adiabaticity in the effective index, attained by the taper structure of SSC, is much influenced by small variation in physical dimensions because of the fineness of the taper structure.

I-L characteristics of SSC-LD is generally different for each facets. As in Fig. 2 slope efficiency from the facet near SSC (front facet) is larger than that from the opposite facet (rear facet). The reason for the different optical output was explained as the nonadiabaticity of the SSC [6]. The variation observed in I-L curves suggests that even in a chip bar SSC's nonadiabaticity varies much from chip to chip. Cho et al. reported that SER depends on the length of nontapered part in SSC-LD [4]. However, their analysis is not applied to the devices in Fig. 2 that are in a chip bar providing devices with the same nontapered active region length.

From Fig. 2, I_{th} and η_{slope} can be extracted for each device (Fig. 3). In the chip bar measured,

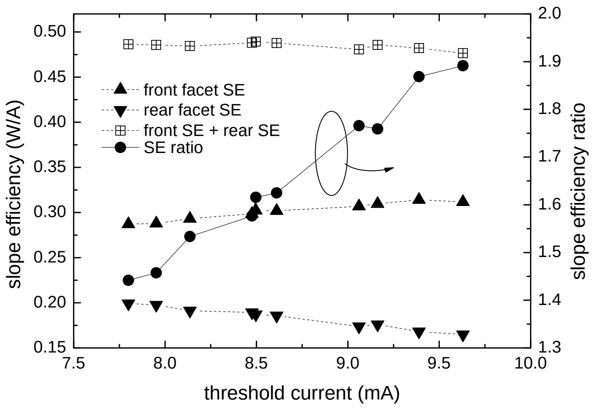

Fig. 3. η_{front}, η_{rear}, $\eta_{front}+\eta_{rear}$, and SER as functions of I_{th}. As I_{th} increases, η_{front} also increases while η_{rear} decreases. This tendency makes SER increases steeply with I_{th}. The opposite behavior of η_{front} and η_{rear} makes $\eta_{front}+\eta_{rear}$ nearly unchanged.

I_{th} of the devices ranges from 7.8 to 8.6 mA. The correlation of I_{th} with η_{front} and η_{rear} is obvious from Fig. 3. As I_{th} increases, η_{front} increases and η_{rear} decreases. This tendency results in steep increase of SER with I_{th}. In this chip bar, SER ranges from 1.44 to 1.89. Due to the opposite behavior of η_{front} and η_{rear}, the total slope efficiency, $\eta_{front} + \eta_{rear}$, seems to be independent of I_{th}, remaining almost unchanged around 0.485 W/A.

η_{slope} is proportional to the photon density at the facet, assuming the difference in effective index is negligible. Therefore the reason for the difference in η_{slope} is different photon density between the two facets. Figure 4 explains why the difference occurs. Among the right-traveling photons with density 1, R is reflected toward the taper at the front facet whose reflectivity is R. All the photons reflected are not coupled to the active waveguide and some of them are lost as radiation. Letting the fraction of the photons recoupled to the active mode be $\alpha(< 1)$, the effective reflectivity of the front facet is $R\alpha$ that is less than R. The existence of the unidirectional loss can, therefore, be interpreted as a low reflectivity coating, resulting in higher η_{slope} of the front facet because photon distribution is concentrated on the vicinity of lower reflectivity facet [8].

Figure 5 is SER of several chip bars versus I_{th}. Horizontal and vertical error bar indicate the standard deviation of I_{th} and SER, respectively. Devices of each chip bar showed clear tendency similar to Fig. 3. Mean values of the chip bars also show proportionality between I_{th} and SER. Mean SER of SSC-LD chip bars was between 1.2 and 2.0 while I_{th} varies from 7.1 to 10.2 mA, which is much larger than the range of SER in a single chip bar. This shows the large spatial variation of the fabrication process of SSC-LD. η_{front} has mean value between 0.26 and 0.33 W/A that can result in extinction ratio difference exceeding 1dB in direct modulation LD. LD with perfectly adiabatic SSC would have SER=1 and $I_{th} = 6.6$ mA from linear regression analysis plotted in blue line in Fig. 5, coinciding closely with the measured data of non-SSC

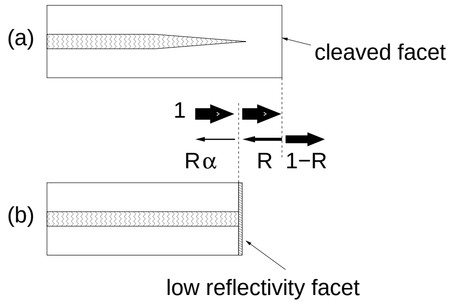

Fig. 4. (a) Schematic plan view figure of SSC-LD. Assuming facet reflectivity R, the fraction of reflected photons among the right-traveling photons is R. As photons propagate further along the SSC region, part of them are lost as radiation and finally $R\alpha$ is coupled to active waveguide mode where $\alpha(<1)$ is the fraction of photons recoupled. (b) Equivalent non-SSC LD is with front facet of reflectivity $R\alpha$.

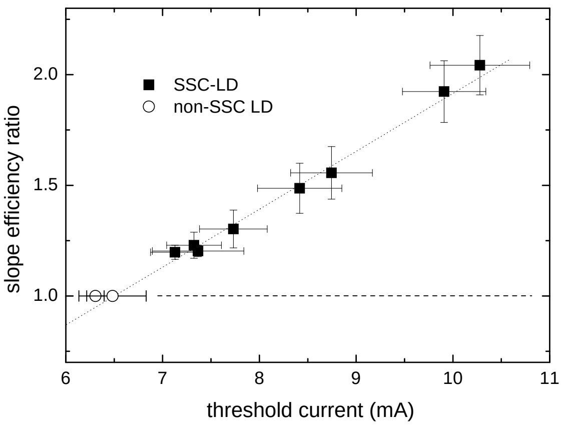

Fig. 5. I_{th} of chip bars versus SER. Each symbol indicates the mean value, and the horizontal and vertical error-bars indicate the standard deviation of SER and I_{th} within a chip bar, respectively. This shows that the trend within a single chip bar (Fig. 3) is also applied between the chip bars. SER=1 means equal output efficiency at both the facets that can be observed from LD without SSC.

LD. However, the coincidence is somewhat accidental because their gain medium property – length, average confinement factor, existence of taper shape, etc. – is different in spite of the same total cavity length.

As far-field is Fourier transform of the near-field, mode expansion is inevitable for narrow beam emission [9]. But the large optical mode expanded is expected to have small recoupling efficiency to the original waveguide unless SSC is perfectly adiabatic. It suggests that far-field angle may be related with η_{slope} or I_{th}. Figure 6 shows horizontal far-field angle (full width at half maximum) of devices in a chip bar as a function of η_{slope}. The far-field angle increases

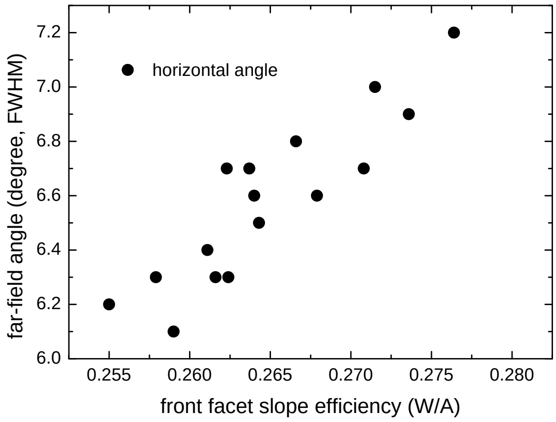

Fig. 6. Horizontal far-field angle of SSC-LD's versus η_{front}. As η_{front} increases, far-field angle also increases. Small far-field angle originates from large near-field mode that causes large unidirectional loss.

from 6.1° to 7.2° with η_{front}. This data shows that LD with large η_{front} has advantage in high optical power transmission owing to both the good coupling and emission efficiency. Because η_{front} is proportional to I_{th}, rather large I_{th} can be the criteria of selecting SSC-LD considering that SSC is adopted in LD for higher fiber-coupled power.

4. Conclusion

SSC integrated BH LD's were fabricated by wet-etching SSC and their I-L characteristics were discussed. The variation in SSC produced during etching process made I_{th} and η_{slope} vary widely compared to non-SSC LD. It was found that η_{front} increases while η_{rear} decreases with I_{th}. SER increases from 1.2 to 2.0 over the wafer while I_{th} increases from 7.1 to 10.2 mA. Far-field angle is also correlated with η_{slope} so that SSC-LD with higher η_{front} has narrower divergence angle. These relations can be explained by unidirectional loss that occurs when photon travels from the front to rear facet.